ADVANCED FUNCTIONAL MATERIALS
www.afm-journal.de

3D Knitting for Pneumatic Soft Robotics

Vanessa Sanchez, Kausalya Mahadevan, Gabrielle Ohlson, Moritz A. Graule, Michelle C. Yuen, Clark B. Teeple, James C. Weaver, James McCann, Katia Bertoldi, and Robert J. Wood**

Soft robots adapt passively to complex environments due to their inherent compliance, allowing them to interact safely with fragile or irregular objects and traverse uneven terrain. The vast tunability and ubiquity of textiles has enabled new soft robotic capabilities, especially in the field of wearable robots, but existing textile processing techniques (e.g., cut-and-sew, thermal bonding) are limited in terms of rapid, additive, accessible, and waste-free manufacturing. While 3D knitting has the potential to address these limitations, an incomplete understanding of the impact of structure and material on knit-scale mechanical properties and macro-scale device performance has precluded the widespread adoption of knitted robots. In this work, the roles of knit structure and yarn material properties on textile mechanics spanning three regimes–unfolding, geometric rearrangement, and yarn stretching–are elucidated and shown to be tailorable across unique knit architectures and yarn materials. Based on this understanding, 3D knit soft actuators for extension, contraction, and bending are constructed. Combining these actuation primitives enables the monolithic fabrication of entire soft grippers and robots in a single-step additive manufacturing procedure suitable for a variety of applications. This approach represents a first step in seamlessly "printing" conformal, low-cost, customizable textile-based soft robots on-demand.

1. Introduction

Pneumatic soft robots can interact safely with fragile bodies, traverse irregular terrain containing environmental uncertainty, and passively adapt to complex object geometries by virtue of their inherent compliance.[1,2] These characteristics have enabled soft robots to capture delicate sea creature samples for study,[3,4] assist people with limited strength for grasping and reaching,[5,6] and have demonstrated utility as remote exploration and inspection devices,[7–10] all while using relatively simple control strategies and, in many cases, the absence of active feedback mechanisms. These strategies rely on the fact that a portion of control is carried out by the materials themselves. Specifically, inherently soft materials, as well as materials structured to become geometrically compliant, can generate necessary actuation forces/pressures that can passively tolerate both task-specific and environmental uncertainty.[2,11]

While early work in soft robotics relied heavily on elastomeric architectures, textiles have emerged as a class of materials that affords a large amount of flexibility for tuning material properties, making them useful as core materials for soft robotic actuation.[12–16] In addition, components made from textiles are lightweight, breathable, and robust to failure modes such as tearing.[15] These beneficial properties contribute to the use of textiles in our everyday clothing and allow scientists to leverage these materials in creating soft robotic garments that are similar in structure and properties to everyday clothes.[6,17–20] However, manufacturing remains a challenge for the development of textile-based soft robots. Currently, cut-and-sew fabrication strategies remain the primary approach used to form textile actuators.[15] This complex and time-consuming manufacturing paradigm relies on human operators, leading to increased system cost and challenges in inter-device uniformity. Cut-and-sew methods also constrain the actuator design space. For example, the heavy reliance on sewing leads to low spatial resolution for patterning, with minimum tolerances in the range of 3–5 mm.[21,22] While bonding of fabrics has been identified as a method for higher-resolution patterning,[12,23,24] these processes have their caveats; due to their use of thermal or chemical adhesion, delamination between layers is a prominent failure mode of the resulting devices. Furthermore, both bonding and sewing are subtractive processes which create waste.

A method to additively manufacture entire soft robotic components on demand, directly from a single machine, could

V. Sanchez, K. Mahadevan, G. Ohlson, M. A. Graule, M. C. Yuen, C. B. Teeple, J. C. Weaver, K. Bertoldi, R. J. Wood
John A. Paulson School of Engineering and Applied Sciences
Harvard University
29 Oxford St., Cambridge, MA 02138, USA
E-mail: vsanchez@seas.harvard.edu; rjwood@seas.harvard.edu

V. Sanchez, J. C. Weaver, R. J. Wood
Wyss Institute for Biologically Inspired Engineering
3 Blackfan Cir., Boston, MA 02115, USA

V. Sanchez
Department of Chemical Engineering
Stanford University
443 Via Ortega, Stanford, CA 94305, USA

J. McCann
Robotics Institute
Carnegie Mellon University
5000 Forbes Ave., Pittsburgh, PA 15213, USA

The ORCID identification number(s) for the author(s) of this article can be found under https://doi.org/10.1002/adfm.202212541.

DOI: 10.1002/adfm.202212541

address all of the aforementioned issues. 3D knitting stands out in this regard due to its capability to create shapes that (i) are tunably compliant along engineered directions with spatially-designed stiffness at high resolutions (as small as the individual stitch level), (ii) integrate multiple materials, including active components, at the yarn level, and (iii) create complex 3D shell shapes, including but not limited to branched tubes,[25,26] all while using only the necessary materials and without generating waste. Specifically, knits use geometrically compliant interlooping or interlaced stitch architectures to form a variety of flexible and stretchable bulk materials, even when the constituent yarns are inextensible.[2,15] Using the capabilities of this technology, researchers have begun to take advantage of knit stitch length differences to shape static inflatable structures[27] and to route integrated cables for actuation.[28] Functional yarns can be knitted to create self-deforming textiles.[29–33] Pneumatic knit systems are beginning to be developed, but complex behaviors (e.g., locomotion) have not yet been demonstrated without additional 3D printed components and assembly,[34] and some motions, such as axial extension, have not yet been demonstrated in any form using pneumatic knit actuators. A more fundamental understanding of knit structures, validated by rigorous experimentation, is therefore necessary to exceed current performance (e.g., in terms of strains, recyclability, multi-degree-of-freedom system integration, etc.) and generate a complete set of actuation profiles (i.e., contraction, extension, bending, coiling) to enable use in real world applications.

To understand the mechanical behavior of knits–which is determined both by interactions between constituent yarns and by the particular interlooping or interlacing stitch architectures used (**Figure 1**b)–researchers have developed models, both data-driven and physics-based.[35–41] However, these models are limited to single structures (i.e., only simple jersey knits) or small strains (e.g., <40%, where recoverable strains for knits can surpass 200% (Figures S11, S15, and S16, Supporting Information)), or they remain constrained to impractical or improbable materials (e.g., only high-bending stiffness monofilaments), which do not translate to the needs of real-world actuators. In the space of computer graphics work on rapid simulation, visually life-like knit fabrics have been explored, but this work is limited to simulation.[42–46] This vast space of knit patterns has also begun to be explored experimentally, but researchers have only characterized small subsets of structures[47–51] or provided databases containing limited characterization data without stress-strain behavior.[52,53] Without stress-strain behavior, there is insufficient information for the design of knit structures for pneumatic actuation. Furthermore,

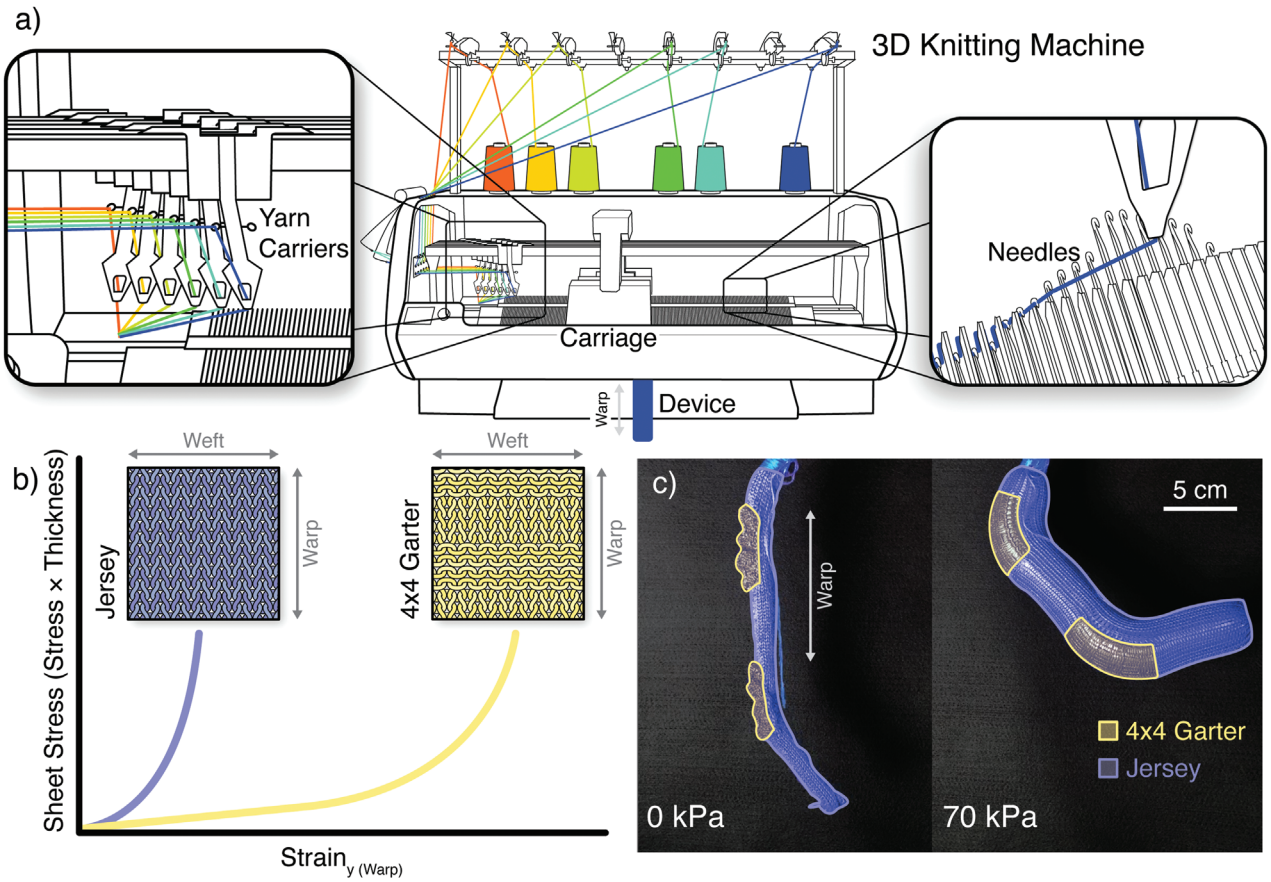

Figure 1. a) The 3D knitting process, in which a knitting machine manipulates multiple yarns simultaneously using mechanical carriers and employs a bed of needles—-the position of each is individually controlled—to interloop one or more of these yarns in a near-infinite set of configurations. b) Resultant knit geometries exhibit starkly different mechanical responses, allowing the mechanical behavior of a knitted manifold to be tuned continuously over its surface. c) For example, by combining jersey and garter knits into one monolithically fabricated soft actuator created in a single step without any human intervention, articulated bending is achieved.

research articles often characterize dissimilar yarn materials knit on different machines (e.g., different style of machine, manufacturer, gauge, etc.) with custom settings (e.g., stitch size, tension, etc.), which makes results incomparable between studies and provides inadequate information to knit monolithic actuators and devices using one knitting machine. There is thus a need for well-characterized knit properties, parameterized across types of knits and constituent yarns of interest, in order to additively manufacture knit soft robots. Specifically, we must unravel the consequences of knit structure and materials on textile stiffness and understand the limitations of tuning parameters within the 3D knitting process in order to develop 3D knit pneumatic actuators that exceed current performance and create devices which rely on several unique independent motion profiles consisting of contraction, extension, bending and coiling.

In this work, we introduce a knitting-based additive manufacturing strategy to design and realize mechanically programmed pneumatic textile-based soft robots in an integrated and monolithic manner. We leverage the unique capabilities of an additive manufacturing technique, V-bed weft knitting (known as 3D knitting) (Figure 1a). We characterize the mechanical properties of knits with architectural and materials-based variations and create generalized guidelines. Although there is a near-limitless set of possible knit combinations to tune material stiffness, we focus on a select set of easily implemented approaches that span a large range of material stiffnesses, which rely on self-folding knit architectures and multi-material knitting, all of which can be paired with 3D shell-shaping strategies to create programmed sleeves for pneumatic actuation. While we cannot characterize every possible knit structure, we develop a simplified strategy to allow for quick comparisons between material properties of knit textiles to assist in unification of experimental characterization work across the field, which can be extended to other knit stitch architectures as well as larger scale 3D shapes. Taking advantage of the ability to create areas of engineered stiffness within 3D shell shapes, we demonstrate complex actuator motion, such as directed bending, which can be generated through the topological entanglement of a single yarn (Figure 1c). Motions generated demonstrate usefulness in several applications including grippers, lifters, and an inspection robot. Because of the reliance on mechanical programming, the knit actuators can be unraveled and the yarn reused, and their soft structure allows them to remain planar and unobtrusive in the uninflated state. The methods in this work are translatable to other commercial and manually-operated V-bed knitting machines, allowing for both large-scale and accessible production of soft robotic actuators at low cost.

2. Knitting to Direct Actuation Motion

2.1. Knit Architectures to Tailor Textile Stiffness

To design additively manufactured pneumatic knit actuators, we leverage unique capabilities of the V-bed knitting process and the ability to program material properties through architectural and materials-based methods on a Kniterate-brand V-bed knitting machine (Figure S8, Supporting Information). In a V-bed knitting machine, yarn *carriers* bring yarns to arrays of *needles*, known as the front and back *beds*, as depicted in Figure 1a. The machine actuates the needles and carriers by drawing a *carriage* back and forth across the beds. The carriage selects which needles operate, and–by means of grooves in a cam plate–controls the needle actuation (tuck, knit, or transfer) and its parameters (stitch length) to form knit fabric, where the length of material coming off the machine is known as the warp and the perpendicular direction is known as the weft (Figure 1a,b). The two-bed layout of V-bed knitting machines allows us to create and shape tubes of various diameters and geometries by knitting with both beds in alternating directions. This two-bed layout also allows the machines to create complex knit architectures, for example, fabrics containing both front-bed knit and back-bed knit (called *purl* in hand knitting) stitches. Our approaches to developing fabrics with programmed variations in knit stiffness arise from the observation that changing these knit stitch structures in patterned methods can generate large changes in the stress–strain behavior of the bulk knit fabrics.

The simplest weft knit structure is the "jersey" knit, which only contains interlooping front bed stitches (**Figure 2**a). When stretched, this knit exhibits two mechanical regimes.[36] Knit architecture dominates the first regime: each stitch geometrically reconfigures as yarns slide and straighten to minimize internal stresses. This initial regime manifests as an approximately linear stiffness. Once the reconfiguration is complete (i.e., the yarns have straightened and can no longer slide further), the yarns themselves undergo deformation and their constituent material properties govern the behavior, experienced as strain stiffening. These two regimes make up the distinctive "J-shaped" stress-strain curve of jersey knit structures (Figure 2b). In order to characterize the behavior of the knits, we cycled knit structures in an extension-controlled test to a maximum force of 15 N, and plotted the stiffness as the derivative of sheet stress (which is the product of engineering stress and initial thickness of the knit) with respect to strain (Figure 2d). As observed in our experimental characterization, increasing the length of yarn in each stitch within this jersey structure reduces the stiffness of the initial regime and also delays the onset of the strain stiffening region. This change in stiffness is much more prominent in the weft direction compared to that of the warp direction (Figure 2d), indicating that in a relaxed state, the warpwise legs of the knit are in a more-parallel configuration, which is supported through imaging (Figure S12, Supporting Information). Other experimental datasets have captured similar behavior, but have been limited to lower strains.[37]

A third mechanical regime can be introduced through modifying the knit geometry using stitch reflections. Akin to the "wavy" or "wrinkled" structures observed in relatively inextensible thin films, which contribute minimally to the stiffness of composites until flattened,[54–56] out-of-plane structures in knits must first be unfolded during deformation before stitch level behavior is seen. As observed in jersey knits, where every stitch on the face of the fabric can be considered a front-bed stitch, the 3D curved geometry of the individual stitches[57] causes the material to curl (Figure S13, Supporting Information). When front bed and back bed stitches are combined within one fabric face, the opposing curvature of these reflected stitches causes the fabric to relax into self-folded knit structures (Figure 2a,c). Bands of these stitch reflections maximize folding, compared to random arrangements (Figures S14, S16, and S17, Supporting

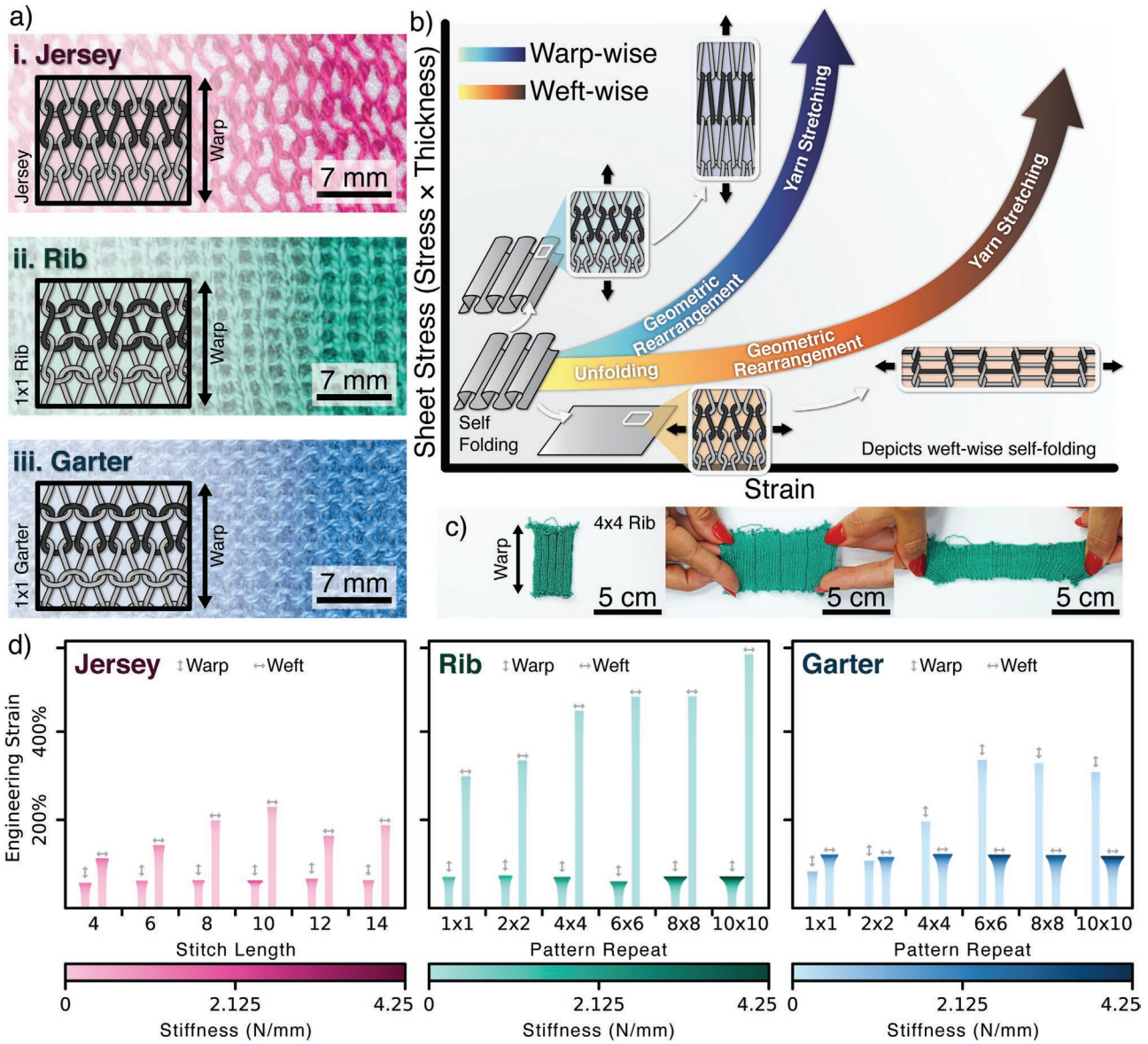

Figure 2. a-i) At its most fundamental level, knitting requires interlooping of yarns, shown here with a simple jersey knit. Asymmetric patterns programmed as varied knit stitch geometries also alters textile properties, and can even introduce sheet-scale wrinkling, folding, and other deformations, as seen in knits created from vertical stitch bands, known as rib a-ii), and horizontal stitch bands known as garter a-iii) (garter fabric photograph recolored uniformly for labeling). These folds and deformations, when present, are typically the primary contributors to overall mechanical behavior during initial deformation b); after unfolding, or in the case of textiles without preprogrammed folds, the yarns themselves next reconfigure geometrically, after which the apparent modulus increases rapidly once the yarns become taut and begin to stretch. Unfolding and subsequent geometric rearrangement are shown in the photographs in c). We characterized 18 different knit structures to create a library of mechanical properties to facilitate the selection of suitable structures when designing knitted robots. A knit's stiffness in response to strain is a key criterion in this design process. The stiffness (obtained as the derivative of sheet stress with respect to strain) as a function of strain is shown in d). For each knit architecture (shown along the x-axis), the stiffness is indicated by the shading and bar width at the given strain (along y-axis). The maximum strain value varies because all samples were cycled to the same maximum force of 15 N and behaviors such as self-folding greatly alter the dimensions of knits which have the same number of stitches (Figures S16 and S17, Supporting Information).

Information). Softness, conceptually akin to the inverse of stiffness, is generated in the fabrics using these bands (known as *rib* when the bands of folds are parallel to the warp direction, and *garter* when the bands are perpendicular to the warp direction). We characterized a representative set of ribs and garters, balanced to reduce edge curling, in the 1 × 1, 2 × 2, 4 × 4, 6 × 6, 8 × 8, and 10 × 10 configurations, where 1 × 1 represents a single unit cell containing one row or column of front knits and back knits (Figure S15, Supporting Information). As illustrated in Figure 2d, increasing the amount of stitches within bands increases the length of the unfolding regime, therefore delaying the onset of the strain stiffening region; the stiffness of the resultant fabric in the direction perpendicular to the bands decreases non-monotonically.

2.2. Knit Architecture-based Motion Primitives

Using the unique mechanical properties of knitted architectures illustrated in Figure 2, we demonstrate seamlessly knit sleeves as primitive motion-based building blocks for contraction, extension, and bending. For example, to form a contraction actuator with its length parallel to the warp-wise direction, knit stitch architectures which are much softer in the weft direction than the warp can be used so that inflation shortens the actuator. In contrast, for warp-wise extension actuators, knit architectures that exhibit softness parallel to the warp-wise direction can be used. For bending actuators, a mechanical mismatch of properties around the actuator's length-wise direction can be selected with the level of mismatch tailored to achieve a specific bending profile or performance. Based on our library of knit architectures, we select knit structures with the aforementioned properties to form monolithic motion primitive actuator sleeves which create the desired motions when an internal bladder is inflated. The actuators were characterized at slow speeds to understand their motion with respect to the quasi-static stress-strain behavior of the textile structures.

In order to automate the fabrication of these actuator sleeves, the Kniterate knit3D library[58] was developed and used to program structures within 3D tubes. As first demonstrated by Paynter in the 1980s and modeled further by Ball and colleagues in 2016, contraction actuators can be formed using jersey knitted warp-wise tubes (**Figure 3**a), similar to braided McKibben actuators.[59,60] These knitted contraction actuators can have a higher actuation stroke at lower forces compared to McKibben actuators.[59,60] Beyond simple contraction actuators made from jersey stitches, which rely on geometric reconfiguration, prior work has not developed the use of varied structures to alter pneumatic actuation behavior. Here, we demonstrate that other structures can achieve superior contraction behavior. For this purpose, we developed a contracting 1×1 rib actuator (Figure 3b). Similar to pleated pneumatic artificial muscles

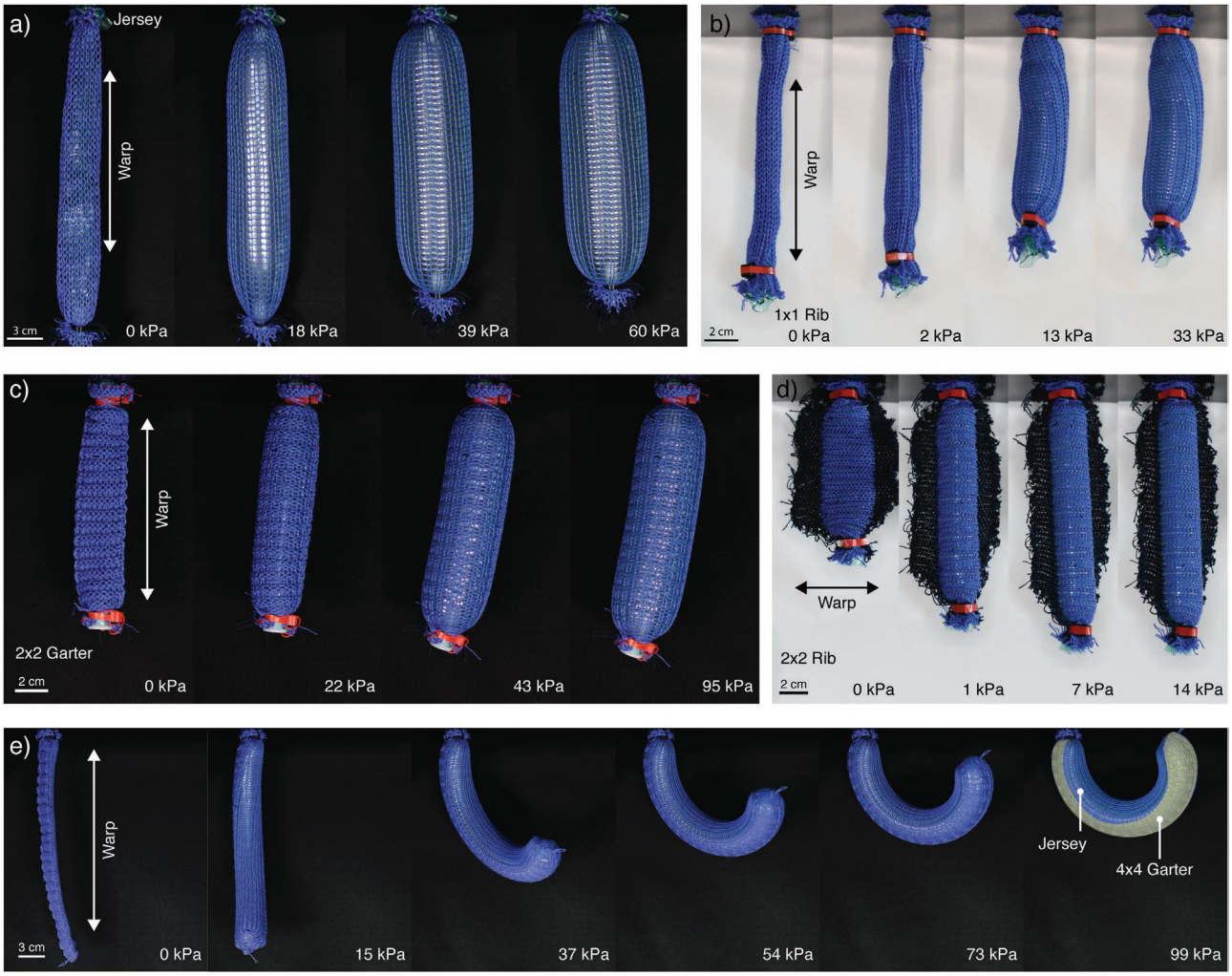

Figure 3. Actuators exhibiting motion primitives (extension, contraction, and bending) can be knit in a single step on the 3D knitting machine. a) A jersey knit tube contracts when inflated using a gas-impermeable internal bladder, but it is outperformed by a rib knit b) as expected based on the mechanical properties of each knit architecture. Knitting a tube in garter, in which folding occurs orthogonally to the folds in rib knits, exhibits extension upon inflation c). Similarly, rotating a rib knit 90 degrees such that its warp direction is perpendicular to the direction of intended actuation also generates extension d). Extending these concepts to arbitrary placement of regions of contraction and extension, in this case by using jersey and garter on opposite sides of a tube knit in a single fabrication process without human intervention, enables bending e).

which rely on unfolding of vertical pleats,[61] we hypothesized that the self-folding nature of the rib structure would unfold preferentially to support contraction. An interesting feature of this rib-knit-based actuator is that the pressure-contraction behavior follows a markedly different response curve than that of a jersey actuator (Figure S19, Supporting Information). Such differences in pressure-motion dependence suggest paired actuators in an integrated device could potentially achieve complex motions with a single pressure input.[62–64]

While knit contractile actuators have been shown in prior work (and improved upon using new knit structures in this work), to the best of our knowledge, knit extension actuators had not yet been demonstrated. In contrast to jersey structures, where the weft is much softer than the warp direction, we hypothesized that changing the weft to be stiffer would cause actuator extension in tubes formed in the warp-wise direction. Based on our library of knits generated in this work, garter structures appeared to be ideal candidates; therefore, we created a 2 × 2 garter tube formed in the warp-wise direction, which created an actuator that extended axially when inflated (Figure 3c). As rib structures in the weft-wise direction are much softer than their garter counterparts with respect to their warp-wise direction, we also illustrated that an extending tube actuator can be created in the weft-wise direction. The resulting rib-based actuator expanded at notably lower pressures relative to the garter-based version (Figure 3d; Figure S18, Supporting Information).

As demonstrated in prior work on pneumatic textile actuators made through cut-and-sew processing, differences in material stiffness can be used to create bending motions.[13,65] With information from our knit mechanics library, bending actuators can be created seamlessly, without cut-and-sew steps, by pairing different knit architectures together within one shell shape (Figure 3e). To demonstrate this concept, a vertically formed bending tube was created from a monolithic combination of jersey and 4×4 garter structures (Figures 1c and 3c).

2.3. Material Variations to Tailor Knit Stiffness

Modifying the yarn material used in knitting can in turn alter the transition points between mechanical regimes. This material-based stiffness tuning is possible because the structural regimes are material-dependent, which occurs because strain, friction, and the ability to bend the yarn around the needles all vary during the knitting process, and therefore the end knit fabric stiffness also varies, even when using the same machine parameters. For yarns with low bending stiffnesses that are relatively inextensible, these regimes follow the previously described pathway of unfolding followed by geometric configuration of the stitches, and finally yarn deformation; however, using extensible yarns will alter the stress–strain curve by changing when the fabric experiences these different regimes. Using elastomeric yarns that are already stretchable in their pre-knit state (Figure S2 and Table S1, Supporting Information) can alter the mechanical behavior significantly. Machine components tension and deform the yarn substantially during the knitting process.[42,66] When the forces are removed after the knit is complete, the resulting fabric will relax substantially, causing the yarns to jam. Our data highlights that, for

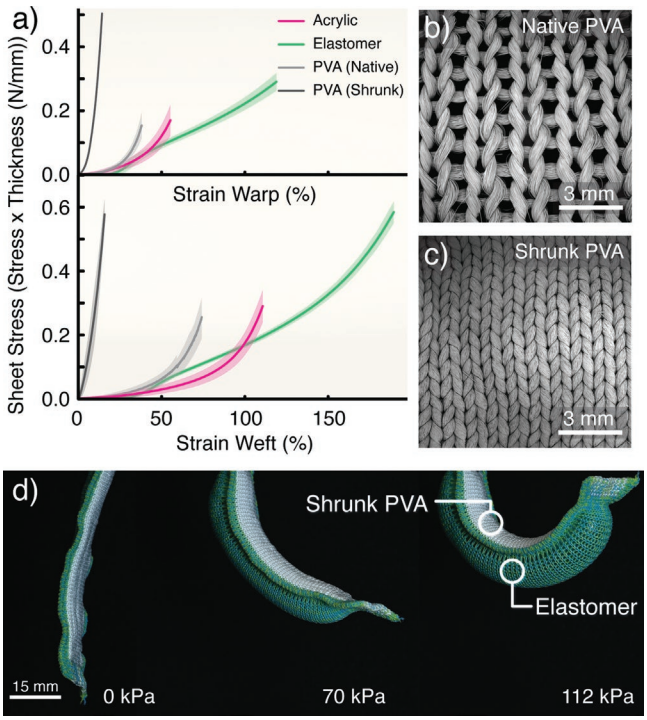

Figure 4. Knits in jammed configurations have substantially different behavior than standard loosely knit yarns. a) Elastomeric yarns which are jammed have an initially stiffer linear onset as geometric reconfiguration is inaccessible, even though the constituent material exhibits a lower modulus than acrylic (Table S1, Supporting Information). Furthermore, postprocessing, and thus jamming, a shrinking PVA yarn creates a much stiffer material; even though the constituent yarn has a lower modulus after processing (Figure S3 and Table S1, Supporting Information). SEM Image b,c) shows how postprocessing PVA yarn with water creates a jammed jersey knit. These material properties can also be beneficial to program actuation motion as shown in a bending actuator created using shrunk PVA and elastomer on either side d).

knits fabricated from these elastomeric materials, stress-strain anisotropy is reduced substantially and the resultant fabrics are initially stiffer than those made from relatively inextensible yarns (**Figure 4**a). This difference arises because the structure of jammed fabrics knit from stretchable yarns hinder geometric rearrangement in the relaxed state, and the yarns themselves must be stretched earlier in the deformation pathway.

Jammed knits can also be generated in a more permanent manner. A key challenge in developing knitted actuators is in preventing unwanted expansion either to use as rigid islands for control components or to direct motion. Post processing strategies can use jamming to quell the geometric rearrangement that is characteristic of knits. We investigated the use of PVA-based yarns that shrink when immersed in water to increase material stiffness. As illustrated in Figure 4a, the stiffness after shrinking increases, while the yarn stiffness itself decreases (Figure S3 and Table S1, Supporting Information), indicating that this change is due to fabric-level structural changes. Through SEM imaging, we investigated the morphology of the shrunken textile, illustrating that in addition to shrinkage, the structure is jammed and not bonded (Figure 4b,c).

Akin to using knit architectures for actuation motion, these material-based strategies can be paired with 3D knitting. We

demonstrate their use in forming a motion primitive bending actuator made using elastomeric yarn on one side and post-processed (i.e., shrunk) PVA yarn on the other (Figure 4d).

2.4. Consequences of Knitting Strategies

All of the actuators and devices presented in this work used sleeves knit monolithically on a V-bed knitting machine to program motion (Movie S1, Supporting Information). When bladders are inserted into these sleeves and inflated, the engineered stiffness of the constraining knit sleeves programs actuator trajectories. Multiple strategies of tuning knit stiffness in the warp and weft directions have been presented here, and when pairing these with 3D knitting, some considerations need to be made. For example, the process of *half-gauging* holds loops of yarn on every other needle, allowing the creation of varied knit stitch architectures with front and back bed knits within knit tubes and other 3D shells (Figure S11, Supporting Information).[67] Half-gauging is typically a reliable process; however, this method reduces machine efficiency because more carriage passes are required to transfer stitches for storage, and it increases the potential for manufacturing defects due to the additional transfers required. If a half-gauge fabric is knit at the same settings as full gauge, the added distance between needles will create a less dense fabric with longer stitch lengths. As sparse textile pneumatic actuators are less robust,[68] in our actuators, we opted to *plait*, or knit two ends of the same yarn together as one, when knitting in half gauge to increase fabric density.

Multi-material knitting allows for yarns with varied mechanical and chemical properties to be incorporated into one textile sleeve. Yarn carriers act as a finite resource within a machine, and can therefore become a constraining factor in device fabrication. An additional carrier is required for each completely unconnected block of material (even from the same base yarn) and for each unconnected closed tube or branch formed in the warp-wise direction (Figure S20, Supporting Information). With the actuators and devices presented in this article, this limitation was not an issue, but looking toward the future in complex integrated soft robots with distributed actuation and sensing, it foreshadows a challenge to automate monolithic manufacturing. Furthermore, differences in material properties can create challenges in transitions between materials; for example, direct transitions from PVA yarn to acrylic often led to manufacturing defects at the interface, so rows of elastomeric yarns were employed to ease joining these two dissimilar materials together. Finally, when considering waste, some materials can be challenging to unravel, such as the highly jammed elastomer and postprocessed PVA, and the use of multiple yarn types creates complexity in separation for recycling.

After removal from the knitting machine, fabrics relax into a minimal energy configuration, which varies based on the structure and material–different fabrics can relax quite distinctly. Short rowing (i.e., knitting on a subset of needles in the row to create additional vertical stitches at specific locations) can be used to account for vertical differences between structures, while increases and decreases (i.e., knitting on more or less needles, using appropriate transferring of stitches) can account for horizontal differences. There are limitations to the number of short rows or increases and decreases that can be performed successfully, however. In short row knitting, especially when knitting tubes, local buildup of material can affect global tension on the knit device; considering decreases, for instance, needles may not have enough space to hold several stacked stitches. When shifting needlebed position (known as racking) for transfers in these states, elevated tension on yarns spanning both beds may cause these yarns to break or stitches on nearby needles to drop. To allow for design guidelines for the development of soft pneumatic actuators considering these constraints, high level generalized features of each of the aforementioned strategies of engineering stiffness are shown in **Table 1**.

3. Application Demonstrations

We demonstrate the versatility of this platform to additively manufacture several soft robotic devices including three soft grippers, a locomotive inspection robot, a high-aspect-ratio coiling actuator, and a self-sensing actuator. All device designs leveraged information from our library of material properties and their compatibility with 3D knitting processes.

A toroidal gripper was created from a combination of yarn materials and knit architectures in a design engineered to ensure multiple points of compliant contact. The edge sections connected to the robot arm fixture were made from stiff PVA shrinking yarn sheets for stability. The ability of 3D knitting to create branched tubes that disconnect and rejoin allowed for the toroidal shape to be created. The actuated hollow toroidal structure was made from acrylic yarns to make use of knit architectural differences; tube sections parallel to the elongated toroid "hole" were formed using a 1×1 rib to leverage their weft-wise expansion to constrain objects, and sections perpendicular to the hole were made from jersey. Between the edge of the PVA section and the hollow branched tube portions, several rows of two ends of elastomeric yarn were used to allow for a smooth transition between dissimilar materials (i.e., PVA and acrylic). The toroidal gripper was able to grasp and hold a wide variety of object shapes and weights (**Figure 5**a and Movie S2,

Table 1. Overview of stiffness-tuning strategies studied in the context of 3D knitting.

	Self-Folding Architectures	Stitch Length Variations	Elastomeric Yarns	Yarn Post-Processing (shrinking)
Additional Carriers Needed	No	No	Yes	Yes
Relaxation Dependent (i.e., short-rowing or increases/decreases required)	Yes	Yes	Yes	Yes; but, relaxation occurs after post-processing
Half-Gauging Required	Yes	No	No	No
Material Accessibility (cost, availability)	High	High	Moderate	Low

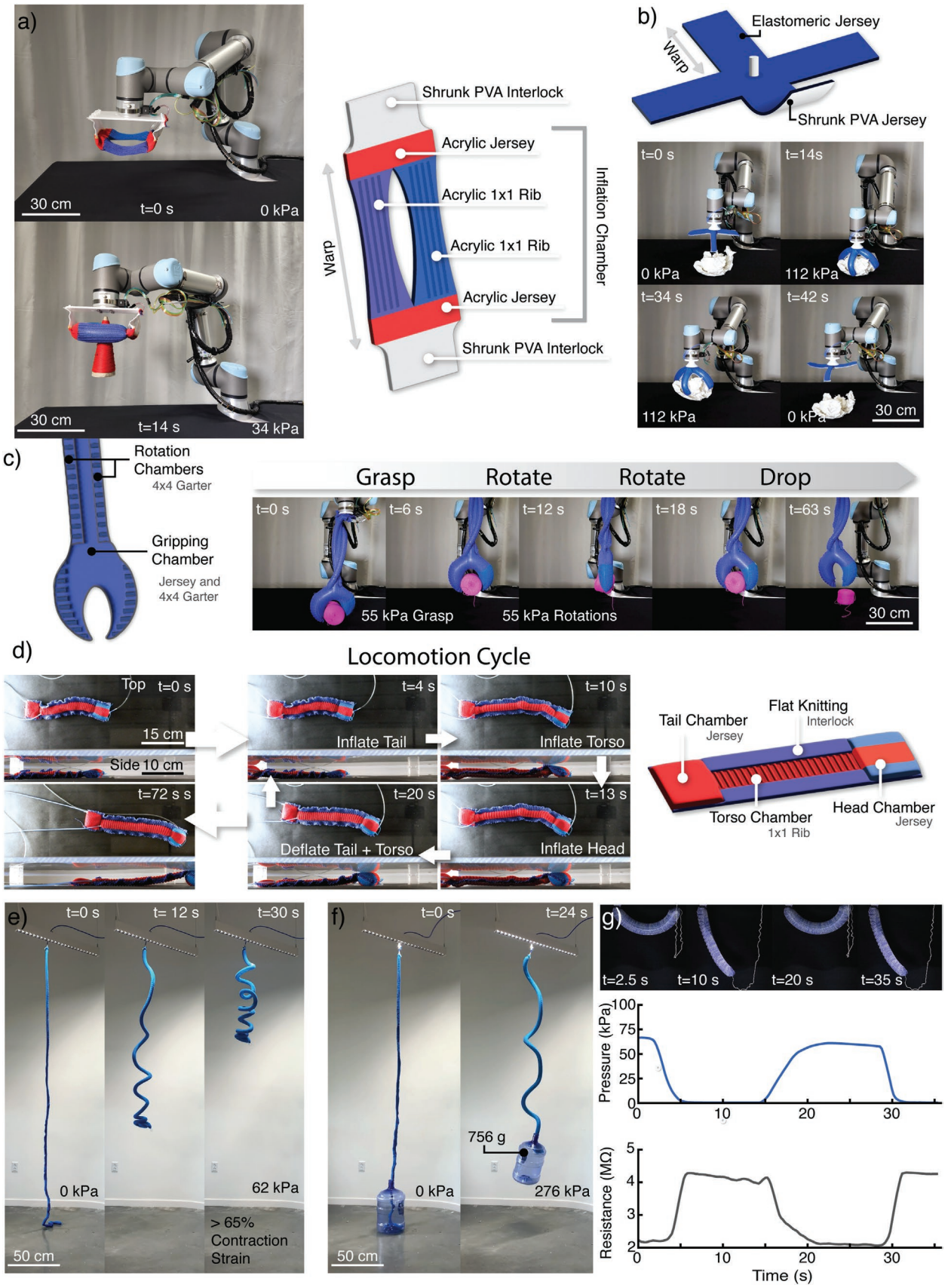

Supporting Information) due to its ability to conform to the object shape.

More "extreme" branched tubes can be leveraged for grasping as well. We demonstrate an X-Gripper containing right angle branches which makes use of two dissimilar materials (i.e., elastomeric yarn and post-processed (shrunk) PVA) knit on the front and back beds of the machine. When actuated, the softer elastomeric yarn expands, allowing for all legs to bend simultaneously and grasp a crumpled paper ball, as illustrated in Figure 5b and Movie S3 (Supporting Information).

In the knitting process, separate actuation chambers can be engineered into monolithic soft robots, including those containing branched shaping. We specifically leverage the use of low numbers of courses and wales (i.e., 1–2 units tall or wide) of a multi-bed interlock structure (Figure S21, Supporting Information) to segment chambers. We demonstrate this capability by creating a rotating claw gripper which contains three distinct chambers. The claw was knit with its length parallel to the warp direction. The claw body was constructed from jersey, and 4×4 garter was used at the sides of the claw for creating bending for grasping motions. The claw contained a connected arm, with two additional chambers separated from the claw body. On these separate chambers, a 4×4 garter was also used at the edges for directed twisting (from anisotropically lengthening edges). These chambers could be actuated individually for grasping, as well as subsequent directed rotation (Figure 5c and Movie S4, Supporting Information).

In addition to grasping, other applications can be achieved by 3D knit soft robots; soft robots able to traverse through small spaces can be used for search and rescue, inspection for areas in need of repair, and exploration.[2,10] We created a soft inspection robot, programmed through monolithic knitting from acrylic yarns through the previously described multi-chamber methods, to create three distinct chambers for locomotion. These chambers include a jersey "head" and "tail" which expand relatively isotropically to lock their positions within a constrained environment, and a highly anisotropically extending 1×1 rib torso to propel the robot forward by changing the displacement between the head and tail. The ability to form these separate chambers with distinct structures and actuate them sequentially enables the robot to move through a small space (42 mm tall) as illustrated in Figure 5d and Movie S5 (Supporting Information).

High aspect ratio pneumatic actuators with complex motions (e.g., bending and coiling) can be challenging to fabricate, and several specialized methods of forming these robotic components have been demonstrated recently in the literature.[1,69,70] Simultaneously, large-scale actuators have been noted as an area of interest for new applications in industrial soft robotics, but face challenges when made from heavy elastomers, pushing development based on fabric materials and manual fabrication methods.[71,72] We demonstrate a coiling and contracting actuator developed with an aspect ratio of 100 by using two knit architectures with disparate stiffness in the warp direction, the same as in Figure 3e, in a lengthened global design. We hypothesize that much larger knit soft robots beyond those demonstrated are quite feasible; in the knitting process, high aspect ratio actuator width is limited by the size of the needle bed. Length (warp-wise dimension), however, is less constrained, and defined by the number of courses knit along with stitch size (at the cost of increased sparseness) (Figure S12 and Table S2, Supporting Information). Although yarn cones are finite, yarns can be tied together when a cone runs out with minimal impacts to the fabric uniformity. The high aspect ratio actuator could coil and contract (Figure 5e and Movie S6, Supporting Information) and achieve >65% free contraction strain at a pressure of 62 kPa. Previous knit contraction actuators, relying on only the jersey architecture, have achieved a maximum of 51% contraction strain at an elongated initial length (i.e., not a length prescribed by the actuator's deformation under only its own weight, but an initial length prescribed by being deformed using an external force).[60] This high aspect ratio actuator could both grasp and lift objects when using higher pressures (Figure 5f and Movie S6, Supporting Information). Our device weighs 87 g, including connection hardware, and is able to lift a five gallon jug weighing 756 g (8.7 times actuator weight), while remaining compact in its unused state.

Finally, we highlight that programming knit actuator motion predominantly using knit stitch architectures, as opposed to material differences,[34,73] is especially amenable to actuators with integrated self-sensing capabilities. By considering the constituent materials' effects on mechanical regimes, resistive deformation sensing can be thoughtfully designed into actuator structures. Previous research using plaiting of elastomeric sensing yarns (specifically those based on conductive particle separation, which result in increased resistance with applied strain) with passive yarns into a knit fabric for strain sensors did not yield significant improvements in sensor behavior compared to a knit formed only from sensing yarn alone.[74] However, we hypothesized that plaiting a spun composite sensing yarn exhibiting decreased resistance with strain (in contrast to the above sensing mechanism)[75] with an insulating yarn would perform well because intra-conductor contacts could be further engineered. Specifically, we plaited blended conductive yarns with passive acrylic yarns for a self-sensing actuator. In addition to practical considerations (e.g., less of an expensive specialty yarn is used, while allowing for a dense knit structure that reduces rupture-based failures as described in McKibben actuators[68]), this method can support a sensor that tracks the internal pressure in the actuator (Figure 5g and Movie S7, Supporting Information).

Figure 5. Demonstrations leveraging 3D knit actuators and devices. a) A knit toroidal gripper made from branched tubes can grasp a variety of objects including a cone of yarn. b) More extreme branched tubes paired with multi-material knitting create a cross gripper which uses bending appendages to grip. c) A multi-chamber claw relying on different knit architectures can grip as well as perform directed rotations based on which chambers are inflated. d) A multi-chamber knit inspection robot uses differences in knit architectures to sequentially anchor the extremities against the external surroundings and extend and contract the body for movement. e) A high-aspect-ratio 3D knit actuator made from two structures can coil to outperform existing tubular knit actuators in contraction. f) This same high aspect ratio actuator can coil within a small-necked jug, much heavier than the actuator itself, to grasp and lift at a higher pressure. g) Plaiting with conductive yarn is amenable to knits using different structures for motion and can be used to track inflation pressure.

4. Conclusion

The use of 3D knitting for soft robots is an emerging research area, yet there have been few quantitative studies on how to tune actuation motion. The ability to structure knits at several scales–from stitch geometry and material to self-folding structures–allows for a variety of mechanical properties and behavior. We have demonstrated a wide array of strategies and structures in this work, and we show how these strategies can be leveraged to generate knit actuation motions not yet demonstrated in extensional actuators, to improve performance beyond the state of the art (e.g., a high-aspect ratio coiling contraction actuator), and to monolithically form complex, multi-actuator devices, such as a fully integrated inspection robot. Furthermore, we have demonstrated that sensing can be paired with these strategies in a knit bending actuator with the ability to track its pressure. Our focus on how knit materials and structures lead to mechanical properties and how these features are compatible with the 3D knitting process enables new design rules engineers and materials scientists can build on. As such, this work represents a step toward generalizing and standardizing the capabilities of knitting as a waste-free additive manufacturing approach capable of monolithically generating soft robots and other useful actuators and devices.

5. Experimental Section

Several yarns were used in this work and were detailed in the text; specifically, knit mechanical property samples were created with 16/2 Vybralite Acrylic Yarns, National Spinning Co. (Peter Patchis Yarns, USA), elastomeric yarn samples were produced using two ends of Yeoman Yarns Elastomeric Nylon Lycra (Yeoman Yarns, United Kingdom) plaited together (i.e., knit together as one yarn), made from 81% nylon and 19% Lycra (a brand name of spandex), Solvron SHC 750 dtex three-ply yarn (Nitivy Co. LTD, Japan) made from 100% polyvinyl alcohol (PVA) was used as a shrinking yarn and shinking post-processing of the PVA yarn was performed by soaking the yarn in 46° water for 5 min, and finally, one end 50/2 and one end of 50/3 Bekinox conductive yarn (Beakart, Belgium) each consisting of the same composition of 80% steel and 20% cotton, plaited together as one yarn with one end of previously described acrylic Vybralite yarn was used for the self-sensing actuator. Further information on yarn construction and tensile properties, tested using an Instron universal testing machine, are included in Supporting Information.

All samples were knit on a Kniterate V-bed knitting machine (Figure S8, Supporting Information) (Kniterate, EU) using the aforementioned yarns. All stress–strain testing of knit architectural and materials samples was performed using Instron universal testing machines using specialized grips (Figure S10, Supporting Information) to prevent slippage. Unless otherwise stated, knitting was performed at standard full gauge settings where lateral tension was kept at 100% and upper yarn tension was maintained at 50%, takedown roller movement was set to 5.71 mm (400 units in Kniterate-specific machine roller values), knitting speed was set to 0.88 m s^{-1} (400 units in Kniterate-specific machine speed values), stitch size was set to four, and transfer speed was set to 0.66 m s^{-1} (300 units in Kniterate-specific machine speed values). These settings were empirically tuned to successfully produce samples and minimize manufacturing defects. To create double bed knit architectures within 3D knitted shells, half gauge knitting was required.[67] All half gauge knitting was performed in standard half gauge settings of a stitch size of five with roller motion setting set to 6.42 mm (450 units) using two ends of acrylic Vybralite yarn to create a dense fabric, unless otherwise specified. These settings were empirically tuned to prevent manufacturing defects.

Programming for all stress–strain samples was performed using the Python frontend[76] of the Knitout Specification.[77] 3D knit actuator motion was programmed using the Kniterate knit3D library developed for this project[58] and Python scripts written using the Knitout Python frontend.[76] The Kniterate-specific backend[78] was used to convert the Knitout programs to "kcode" (a lower level machine language usable by the Kniterate knitting machine). All Knitout code is included in the 3Dknit_softrobots Github Repository.

To form air-tight pouches to pressurize the 3D knit soft robots, oversized sealed bladders made from Strechlon 200 film (Fibre Glast, USA) were formed using previously demonstrated methods[13,79] and inserted into knit sleeves. Bladders were connected to tubing and closed using barbed fittings, cable ties, and Silpoxy adhesive (Smooth-On Inc., USA). Complex 3D actuators with integrated bladder insertion holes had holes closed manually using the same yarn.

To evaluate all motion-primitive actuators, Images were taken with a DSLR camera at static set pressures and pressure was measured using a high-resolution digital gauge (MGA-30-A-9V-R, SSI Technologies LLC).

Ethics Approval Statement

All people photographed and videotaped in this manuscript and the Supporting Information consent to having their images and videos published.

Supporting Information

Supporting Information is available from the Wiley Online Library or from the author.

Acknowledgements

G.O. and M.A.G. contributed equally to this work. This material was based upon work supported by the National Science Foundation under grant no. EFMA-1830901 for the EFRI program, grant no. DMR-1420570 for the Harvard MRSEC REU Program, grant no. 1955444 for the HCC program, and grant no. DMR-2138020 for the MPS-Ascend program. Research was sponsored by the Army Research Office and was accomplished under grant no. W911NF-22-1-0219. The authors also acknowledge support from the Wyss Institute for Biologically Inspired Engineering and the Harvard John A. Paulson School of Engineering and Applied Sciences. V.S. acknowledges salary support from the National Defense Science and Engineering Graduate Fellowship, as well as from the National GEM Consortium through the GEM fellowship. The authors would like to thank Dr. Perrin Schiebel and Dr. Oluwaseun Araromi for discussions. Any opinions, findings, and conclusions or recommendations expressed in this material were those of the authors and do not necessarily reflect the views of the National Science Foundation.

Conflict of Interest

The authors declare no conflict of interest.

Data Availability Statement

All data pertinent to this study are included within the main manuscript or the supporting information and are also available from corresponding authors upon reasonable request. Knitout program files used to fabricate samples of knit structures, motion primitives, and 3D knit soft robot demonstrations have been deposited in

GitHub and are publicly available to download at: https://github.com/harvard-microrobotics/3Dknit_softrobots.

Keywords

additive manufacturing, metamaterials, pneumatic actuators, soft robotics, soft sensors, textiles

Received: October 28, 2022
Revised: February 26, 2023
Published online: April 23, 2023

[1] K. Becker, C. Teeple, N. Charles, Y. Jung, D. Baum, J. C. Weaver, L. Mahadevan, R. Wood, *Proc. Natl. Acad. Sci.* **2022**, *119*, e2209819119.
[2] B. Jumet, M. D. Bell, V. Sanchez, D. J. Preston, *Adv. Intel. Syst.* **2022**, *4*, 2100163.
[3] N. R. Sinatra, C. B. Teeple, D. M. Vogt, K. K. Parker, D. F. Gruber, R. J. Wood, *Sci. Rob.* **2019**, *4*, eaax5425.
[4] K. C. Galloway, K. P. Becker, B. Phillips, J. Kirby, S. Licht, D. Tchernov, R. J. Wood, D. F. Gruber, *Soft Rob.* **2016**, *3*, 23.
[5] H. K. Yap, P. M. Khin, T. H. Koh, Y. Sun, X. Liang, J. H. Lim, C. H. Yeow, *IEEE Robot. Autom. Lett.* **2017**, *2*, 1383.
[6] C. Simpson, B. Huerta, S. Sketch, M. Lansberg, E. Hawkes, A. Okamura, *IEEE Trans. Med. Robot. Bionics* **2020**, *2*, 474.
[7] D. Drotman, S. Jadhav, M. Karimi, P. de Zonia, M. T. Tolley, in *Proc. 2017 IEEE Int. Conf. Robot. Autom. (ICRA)*, **2017**, pp. 5532.
[8] W. Adams, S. Sridar, C. M. Thalman, B. Copenhaver, H. Elsaad, P. Polygerinos, in *Proc. 2018 IEEE Int. Conf. Soft Robotics (RoboSoft)*, **2018**, pp 321.
[9] E. W. Hawkes, C. Majidi, M. T. Tolley, *Sci. Rob.* **2021**, *6*, eabg6049.
[10] S. Aracri, F. Giorgio-Serchi, G. Suaria, M. E. Sayed, M. P. Nemitz, S. Mahon, A. A. Stokes, *Soft Rob.* **2021**, *8*, 625.
[11] D. Rus, M. T. Tolley, *Nature* **2015**, *521*, 467.
[12] F. Connolly, D. A. Wagner, C. J. Walsh, K. Bertoldi, *Extreme Mech. Lett.* **2019**, *27*, 52.
[13] L. Cappello, K. C. Galloway, S. Sanan, D. A. Wagner, R. Granberry, S. Engelhardt, F. L. Haufe, J. D. Peisner, C. J. Walsh, *Soft Rob.* **2018**, *5*, 662.
[14] N. D. Naclerio, E. W. Hawkes, *IEEE Robot. Autom. Lett.* **2020**, *5*, 3406.
[15] V. Sanchez, C. J. Walsh, R. J. Wood, *Adv. Funct. Mater.* **2021**, *31*, 1.
[16] N.-K. Persson, J. G. Martinez, Y. Zhong, A. Maziz, E. W. H. Jager, *Adv. Mater. Technol.* **2018**, *1700397*, 1700397.
[17] C. J. Payne, E. G. Hevia, N. Phipps, A. Atalay, O. Atalay, B. R. Seo, D. J. Mooney, C. J. Walsh, in *Proc. 2018 IEEE Int. Conf. Robot. Autom. (ICRA)*, **2018**, pp. 5459.
[18] D. J. Preston, H. J. Jiang, V. Sanchez, P. Rothemund, J. Rawson, M. P. Nemitz, W.-K. Lee, Z. Suo, C. J. Walsh, G. M. Whitesides, *Sci. Rob.* **2019**, *4*, eaaw5496.
[19] M. Zhu, T. N. Do, E. Hawkes, Y. Visell, *Soft Rob.* **2020**, *7*, 179.
[20] J. Fang, J. Yuan, M. Wang, L. Xiao, J. Yang, Z. Lin, P. Xu, L. Hou, *Soft Rob.* **2020**, *7*, 95.
[21] J. Lee, C. Steen, *Technical Sourcebook for Apparel Designer*s, 3rd Ed., Fairchild Books, New York **2019**.
[22] C. M. Thalman, Q. P. Lam, P. H. Nguyen, S. Sridar, P. Polygerinos, in *Proc. 2018 IEEE Int. Conf. Intell. Robot. Syst. (IROS)*, **2018**, pp. 6965.
[23] V. Sanchez, C. J. Payne, D. J. Preston, J. T. Alvarez, J. C. Weaver, A. T. Atalay, M. Boyvat, D. M. Vogt, R. J. Wood, G. M. Whitesides, C. J. Walsh, *Adv. Mater. Technol.* **2020**, *5*, 2000383.
[24] R. Natividad, M. Del Rosario, P. C. Chen, C. H. Yeow, *Soft Rob.* **2018**, *5*, 304.
[25] J. Underwood, *Doctoral Thesis*, Royal Melbourne Institute of Technology (RMIT University), **2009**.
[26] D. J. Spencer, *Knitting technology: A comprehensive handbook and practical guide*, CRC Press, Boca Raton **2001**.
[27] Y. Baranovskaya, M. Prado, M. Dörstelmann, A. Menges, *Complexity Simplicity Proc. 34th eCAADe Conference* **2016**, *1*, 571.
[28] L. Albaugh, S. Hudson, L. Yao, in *Proc. of the 2019 CHI Conf. on Human Factors in Computing Systems*, **2019**.
[29] J. Abel, J. Luntz, D. Brei, *Smart Mater. Struct.* **2012**, *21*, 085011.
[30] J. Abel, J. Luntz, D. Brei, *Smart Mater. Struct.* **2013**, *22*, 125001.
[31] J. Foroughi, G. M. Spinks, S. Aziz, A. Mirabedini, A. Jeiranikhameneh, G. G. Wallace, M. E. Kozlov, R. H. Baughman, *ACS Nano* **2016**, *10*, 9129.
[32] A. Maziz, A. Concas, A. Khaldi, J. Stålhand, N.-K. Persson, E. W. H. Jager, *Sci. Adv.* **2017**, *3*, e1600327.
[33] M.-W. Han, S.-H. Ahn, *Adv. Mater.* **2017**, *29*, 1606580.
[34] Y. Luo, K. Wu, A. Spielberg, M. Foshey, D. Rus, T. Palacios, W. Matusik, in *Proc. 2022 CHI Conf. Human Factors in Computing Systems*, **2022**.
[35] S. Poincloux, M. Adda-bedia, D. Lyon, *Phys. Rev. X* **2018**, *021075*, 1.
[36] S. Kawabata, in *Textile structural composites*, (Eds.: T.-W. Chou, F. K. Ko), Elsevier, New York **1989**, pp. 67.
[37] O. Weeger, A. H. Sakhaei, Y. Y. Tan, Y. H. Quek, T. L. Lee, S.-K. Yeung, S. Kaijima, M. L. Dunn, *Appl. Compos. Mater.* **2018**, *25*, 797.
[38] T. D. Dinh, O. Weeger,, S. Kaijima, , S.-K. Yeung, Compos. B. Eng. **2018,** 148, 81.
[39] D. Liu, D. Christe, B. Shakibajahromi, C. Knittel, N. Castaneda, D. Breen, G. Dion, A. Kontsos, *Int. J. Solids Struct.* **2017**, *109*, 101.
[40] D. Liu, B. Shakibajahromi, G. DIon, D. Breen, A. Kontsos, *J. Appl. Mech. Trans. ASME* **2018**, *85*, 1.
[41] E. Tekerek, D. Liu, B. Wisner, M. Mathew, N. Castaneda, M. Oncul, A. Kontsos, *Mater. Design Process. Commun.* **2020**, *2*, 1.
[42] J. M. Kaldor, D. L. James, S. Marschner, Yeung, *ACM Trans. Graph.* **2008**, *27*, 1.
[43] C. Yuksel, J. M. Kaldor, D. L. James, S. Marschner, *ACM Trans. Graph.* **2012**, *31*, 4.
[44] J. Leaf, R. Wu, E. Schweickart, D. L. James, S. Marschner, *ACM Trans. Graph.* **2018**, *37*, 6.
[45] G. Cirio, J. Lopez-Moreno, M. A. Otaduy, *IEEE Trans. Visual. Comp. Graph.* **2017**, *23*, 1152.
[46] G. Sperl, R. Narain, C. Wojtan, *ACM Trans. Graph. (TOG)* **2020**, *39*, 4.
[47] E. Perumalsamy, J. C. Sakthivel, N. Anbumani, *Int. J. Cloth. Sci. Technol.* **2014**, *26*, 222.
[48] Z. Jinyun, L. Yi, J. Lam, C. Xuyong, *Text. Res. J.* **2010**, *80*, 1965.
[49] E. Fatkić, J. Geršak, D. Ujević, *Fibr. Text. East. Eur.* **2011**, *19*, 88.
[50] D. B. Sitotaw, B. F. Adamu, *J. Eng.* **2017**, *2017*, 7.
[51] B. A. Mcgregor, R. Postle, *Text. Res. J.* **2008**, *78*, 399.
[52] M. Hofmann, L. Albaugh, T. Sethapakadi, J. Hodgins, S. E. Hudson, J. McCann, J. Mankoff, in *Proc. 32nd Ann. ACM Symp. User Interface Software and Technol.*, **2019**, pp. 5.
[53] L. Albaugh, J. Hodgins, M. Hofmann, S. Hudson, J. Mankoff, J. McCann, T. Sethapakdi, Knitdb, https://github.com/textiles-lab/knitdb, (accessed January 2021).
[54] Y. Ma, X. Feng, J. A. Rogers, Y. Huang, Y. Zhang, *Lab Chip* **2017**, *17*, 1689.
[55] W. K. Lee, C. J. Engel, M. D. Huntington, J. Hu, T. W. Odom, *Nano Lett.* **2015**, *15*, 5624.
[56] W. K. Lee, W. B. Jung, S. R. Nagel, T. W. Odom, *Nano Lett.* **2016**, *16*, 3774.
[57] D. L. Munden, *J. Text. Inst. Trans.* **1959**, *50*, T448.
[58] G. Ohlson, knitout-kniterate-3d, https://github.com/gabrielle-ohlson/knitout-kniterate-3D, (accessed January 2022).
[59] H. M. Paynter, High Pressure Fluid-Driven Tension Actuators and Method for Constructing Them, US4751869, **1988**.

[60] E. J. Ball, M. A. Meller, J. B. Chipka, E. Garcia, *Smart Mater. Struct.* **2016**, *25*, 115024.
[61] F. Daerden, D. Lefeber, *Int. J. Fluid Power* **2001**, *2*, 41.
[62] B. Gorissen, E. Milana, A. Baeyens, E. Broeders, J. Christiaens, K. Collin, D. Reynaerts, M. De Volder, *Adv. Mater.* **2019**, *31*, 1804598.
[63] N. Vasios, A. J. Gross, S. Soifer, J. T. Overvelde, K. Bertoldi, *Soft Rob.* **2020**, *7*, 1.
[64] C. C. Futran, S. Ceron, B. C. Mac Murray, R. F. Shepherd, K. H. Petersen, in *2018 IEEE Int. Conf. Soft Robotics (RoboSoft)*, IEEE, **2018**, pp. 473.
[65] Y. Kadowaki, T. Noritsugu, M. Takaiwa, D. Sasaki, M. Kato, *J. Robot. Mechatron.* **2011**, *23*, 281.
[66] L. Kapllani, C. Amanatides, G. Dion, V. Shapiro, D. E. Breen, *Graph. Models* **2021**, *118*, C.
[67] V. Narayanan, K. Wu, C. Yuksel, J. McCann, *ACM Trans. Graph.* **2019**, *38*, 4.
[68] S. Davis, D. G. Caldwell, *Int. J. Rob. Res.* **2006**, *25*, 359.
[69] K. P. Becker, Y. Chen, R. J. Wood, *Adv. Funct. Mater.* **2020**, *1908919*, 1.
[70] T. J. Jones, E. Jambon-Puillet, J. Marthelot, P.-T. Brun, *Nature* **2021**, *599*, 229.
[71] S. Li, S. A. Awale, K. E. Bacher, T. J. Buchner, C. Della Santina, R. J. Wood, D. Rus, *Soft Rob.* **2022**, *9*, 324.
[72] N. Oh, H. Rodrigue, *Soft Rob.* **2023**, *10*, 88.
[73] Z. Liu, X. Han, Y. Zhang, X. Chen, Y.-K. Lai, E. L. Doubrovski, E. Whiting, C. C. L. Wang, *ACM Trans. Graph.* **2021**, *40*, 4.
[74] S. Seyedin, S. Moradi, C. Singh, J. M. Razal, *Appl. Mater. Today* **2018**, *11*, 255.
[75] J. Xie, H. Long, M. Miao, *Smart Mater. Struct.* **2016**, *25*, 105008.
[76] V. Narayanan, J. McCann, knitout-frontend-py, https://github.com/textiles-lab/knitout-frontend-py, (accessed January 2021).
[77] L. Albaugh, J. McCann, Knitout, https://github.com/textiles-lab/knitout, accessed Jan. 2021.
[78] V. Narayanan, G. Ohlson, J. McCann, Knitout-to-kcode backend, https://github.com/textiles-lab/knitout-backend-kniterate, (accessed Junuary 2021).
[79] S. E. Root, V. Sanchez, J. A. Tracz, D. J. Preston, Y. S. Zvi, K. Wang, C. J. Walsh, S. Homer-Vanniasinkam, G. M. Whitesides, *Adv. Mater. Technol.* **2022**, *7*, 2101563.